Dear Author,

Please, note that changes made to the HTML content will be added to the article before publication, but are not reflected in this PDF.

Note also that this file should not be used for submitting corrections.

Catalysis Today xxx (2016) xxx–xxx

Contents lists available at ScienceDirect

Catalysis Today

journal homepage: www.elsevier.com/locate/cattod

Nanosized inorganic metal oxides as heterogeneous catalysts for the degradation of chemical warfare agents

Q1 Chiara Bisio[a,b,*], Fabio Carniato[a], Chiara Palumbo[b], Sergey L. Safronyuk[d], Mykola F. Starodub[c], Andrew M. Katsev[d], Leonardo Marchese[a], Matteo Guidotti[b,**]

[a] Dipartimento di Scienze e Innovazione Tecnologica and Nano-SiSTeMI Interdisciplinary Centre, Università del Piemonte Orientale "A. Avogadro", Viale T. Michel 11, 15121 Alessandria, Italy
[b] CNR-Istituto di Scienze e Tecnologie Molecolari, via C. Golgi 19, 20133 Milano, Italy
[c] National University of Life and Environmental Sciences of Ukraine, Kyiv, Ukraine
Q2 [d] V.I. Vernadsky Crimean Federal University, Medical Academy, Simferopol, Ukraine

ARTICLE INFO

Article history:
Received 12 August 2015
Received in revised form
28 December 2015
Accepted 31 December 2015
Available online xxx

Keywords:
Heterogeneous catalysis
Oxidation
Chemical warfare agents
Organosulfur
Metal oxide
Bioluminescent bacteria

ABSTRACT

Nanosized inorganic metal oxides, such as TiO_2, ZnO, γ-Al_2O_3, are proposed as heterogeneous catalysts for the oxidative degradation of chemical warfare agents (CWA), particularly of organosulfur toxic agents, into oxidised products with reduced toxicity. The morphology, structural and textural properties of the catalysts were investigated. Furthermore, their catalytic properties were evaluated in the oxidative abatement of (2-chloroethyl)ethylsulfide, CEES, a simulant of sulfur mustard (blistering CWA). Their performance was also compared to a conventional decontamination powder and a commercial Nb_2O_5 sample. The metal oxides powders were then employed in the active oxidative decontamination of CEES from a cotton textile substrate, mimicking a real contamination occurrence. Remarkable results in terms of abatement and degradation into desired products were recorded, achieving good conversions and decontamination efficiency with Nb_2O_5, TiO_2 and γ-Al_2O_3, under very mild conditions, with hydrogen peroxide (as aqueous solution or as urea-hydrogen peroxide adduct), at room temperature and ambient pressure. In the aim of a real on-field use, the potential environmental impact of these solids was also evaluated by bioluminescence toxicity tests on reference bacteria (*Photobacterium leiognathi* Sh1), showing a negligible negative impact for TiO_2, γ-Al_2O_3, and Nb_2O_5. A major biotoxic effect was only found for ZnO.

1. Introduction

Q4 Chemical warfare agents (CWAs) have been considered among the most deadly tools humankind has ever invented deliberately. The oxidative abatement of pollutants and toxic chemical warfare agents is conventionally achieved via stoichiometric reactions based on the use of strong oxidants (mainly, sources of active chlorine, such as NaOCl, $Ca(OCl)_2$ or dichloroisocyanurate salts) with high environmental impact and/or via thermal degradation [1,2]. These procedures are often associated with high energy consumption, Q5 large over-stoichiometric amounts of reactants and high costs.

As an alternative to these well-established conventional chemical abatement strategies, and aiming to overcome their limits, many heterogeneous catalysts have been proposed for the selective oxidation of CWAs into partially or fully oxidized non-toxic products [3,4]. For instance, polyoxometalates activated with transition metal centres (i.e. V, Fe, W, Mo) [5,6] and porous oxides, such as zeolite and metal-containing mesoporous silica [7–11], have been studied for these purposes. Typically, these catalysts have shown good conversion and high selectivity values in the oxidation of organic sulfides into sulfoxides, in particular of those compounds that mimic the oxidative abatement of blistering agents. Furthermore, these inorganic solids are characterized by a remarkable chemical, physical and mechanical robustness and, thanks to their high surface area, display a good dispersion of the catalytically active sites.

More recently, phyllosilicate clay materials have also been tested in the abatement of CWA [12,13]. The good chemical versatility and the low production costs render these solids promising

* Corresponding author at: Dipartimento di Scienze e Innovazione Tecnologica and Nano-SiSTeMI Interdisciplinary Centre, Università del Piemonte Orientale "A. Avogadro", Viale T. Michel 11, 15121 Alessandria, Italy.
Q3 ** Corresponding author. Fax: +39 02 50314405.
E-mail addresses: chiara.bisio@mfn.unipmn.it (C. Bisio), m.guidotti@istm.cnr.it (M. Guidotti).

http://dx.doi.org/10.1016/j.cattod.2015.12.023
0920-5861/

candidates for the oxidative degradation of CWAs. A novel Nb(V)-containing saponite clay (Nb-SAP) was prepared by some of us (at the University of Eastern Piedmont, Italy) and identified as an efficient catalyst for the oxidative abatement of blistering agents [14]. The synthesis method used to obtain metal-substituted saponite material was modified to allow the insertion of Nb(V) ions within the inorganic framework of the clay: a bifunctional redox/acid catalyst with strong oxidizing properties, due to the presence of Nb(V) centres [15] and Brønsted acid character, due to aluminium ions embedded into the tetrahedral silica sheets of the saponite clay, was thus obtained [16]. The cooperative effect of the metal centres and the acid sites was crucial to promote the oxidative abatement of organosulfur blistering agents with hydrogen peroxide under very mild conditions and, in particular, with no use of chlorine-containing oxidising reagents. In detail, (2-chloroethyl) ethylsulfide (CEES), an organic compound whose structure and reactivity is similar to sulfur mustard (the blistering agent yperite, used for the first time during World War I), was selectively oxidized to the non-toxic (2-chloroethyl) ethylsulfoxide. The Nb-saponite catalyst was able to convert more than 98% of CEES, with a 73% selectivity to the related sulfoxide in 8 h [14]. Notably, this performance was significantly better than the one obtained over a conventional commercial decontamination powder, based on alumina and calcium hypochlorite.

Besides porous and layered materials, inorganic metal oxides, such as Al_2O_3, TiO_2 and MgO have been also studied for their positive effects on the CWA oxidation and/or degradation reactions [1,17,18]. Often, these solids have been merely used as supports to disperse catalytically active metals, rather than as directly involved catalysts [19–21]. The catalytic decontamination performance of such inorganic oxides is moderate when they are in the form of bulk aggregates or micrometric dispersions, since they are able to remove quite efficiently by physical adsorption the hazardous agent, but then they can degrade it only partially [22–25]. On the contrary, when they are dispersed at nanometric level, their intrinsic acid/base properties and hence their hydrolytic capabilities, which are related to both the chemical nature of the metal oxide and to the surface properties, can be directly exploited for a successful CWA abatement [26–30].

Finally, considering the ever-growing concern about the potential detrimental effects of nanostructured inorganic oxides on living organisms [31,32], it is also necessary to pay a constant attention to the potential risks connected to the use of catalytically-active nanosized solids at large scale. Since the use of nanostructured decontamination powders is envisaged, in the present case, not only for the abatement of CWAs in closed and confined environments, but also in on-field total-loss situations, it is necessary to carry out an estimation of the potential detrimental effects on both living organisms and the environment [33–35].

In this respect, a series of nanostructured inorganic oxides, namely, ZnO with layered morphology, TiO_2 with anatase structure and γ-Al_2O_3, were synthesized and tested in the oxidative degradation of the chemical warfare blistering agent simulant (2-chloroethyl) ethyl sulfide. The first set of reactions was conducted in a batch reactor, under controlled conditions (room temperature), and in the presence of aqueous hydrogen peroxide as an oxidant. A critical comparison of their catalytic properties in relation to their physico-chemical characteristics was also carried out. The second series of reactions was performed on a textile substrate, mimicking a real contamination occurrence, at room temperature, with the urea hydrogen peroxide (UHP) adduct as an oxidant. A difference in reactivity of the catalysts within the two series was registered and is herein described.

In the aim of a real on-field use, the potential environmental impact of these solids was finally evaluated by bioluminescence tests, using reference marine bioluminescent bacteria (*Photobacterium leiognathi* Sh1) as a target.

2. Experimental details

2.1. Materials

Commercial M75CBRN (chemical, biological, radiological and nuclear agent) decontamination powder, packed in sealed batches, was obtained at the local Military Hospital in Milan (Italy) and used as received, as a reference material.

Bulk hexagonal-phase Nb_2O_5 (Aldrich, 99.99%) was used as reference for the catalytic comparison.

2.2. Catalyst preparation

ZnO with nanosheet morphology was prepared by thermal decomposition of the $Zn_4CO_3(OH)_6{\cdot}H_2O$ precursor obtained by chemical bath deposition (CBD), adapting a methodology reported in the literature [36]. 0.55 g of hydrated zinc acetate ($Zn(CH_3COO)_2{\cdot}2H_2O$, Sigma–Aldrich) were added to 3.00 g of urea (Sigma–Aldrich) in 50 mL of deionized water, and the pH value of the solution was adjusted to 4.5 with diluted acetic acid. The solution was transferred in an autoclave and kept at 353 K for 12 h. $Zn_4CO_3(OH)_6{\cdot}H_2O$ in powder form was obtained. The sample was finally heated under air at 673 K to promote the decomposition of $Zn_4CO_3(OH)_6{\cdot}H_2O$ into ZnO.

γ-Al_2O_3 was synthesized by modifying the classical sol–gel procedure that is normally used to produce boehmite phase [37]. In this method, the sol–gel procedure is assisted by sonication in order to reduce the synthesis time. Urea (0.22 g, NH_2CONH_2, Sigma–Aldrich) was dissolved in 30 mL of deionized water. Then, aluminum isopropoxide (3.18 g, $Al[OCH(CH_3)_2]_3$, Sigma) was added to the solution. The obtained gel was stirred at room temperature for 1 h. After this time, the gel was dried at 363 K for 12 h, in order to obtain boehmite precursor, and submitted to a thermal treatment, under oxygen flow (100 mL min^{-1}) at 773 K for 4 h, to promote the phase transition to γ-Al_2O_3.

TiO_2 was prepared as follows. 3.5 mL of titanium(IV) isopropoxide (Sigma–Aldrich) were mixed to 3.5 mL of 2-propanol (Sigma–Aldrich) and the solution was submitted to sonication for 15 min. 8 mL of pure water were added drop-by-drop to the previous solution under slow stirring. The final suspension was sonicated for other 15 min and dried at 353 K overnight. The sample, in form of white powder, was calcined under air flow (100 mL min^{-1}) at 573 K for 2 h.

2.3. Catalyst characterization

X-ray powder diffraction (XRPD) of unoriented ground powders was collected with a Thermo ARL 'XTRA-048 diffractometer using Cu Kα (λ = 1.54 Å) radiation. Diffractograms were recorded at room temperature with a step size of 0.02° and a rate of 1° 2θ min^{-1}. The particle size for the different samples was estimated by using the Debye–Scherrer equation.

Transmission electron microscopy (TEM) images were obtained using a JEOL 3010-UHR instrument operating at 300 kV and a FEI Tecnai F20ST operating at 200 KV. Samples were ultrasonically dispersed in isopropanol and a drop of the suspension was deposited on a copper grid covered with a lacey carbon film.

N_2 physisorption measurements were carried out at 77 K in the relative pressure range from 1×10^{-6} to 1 P/P_0 by using a Quantachrome Autosorb1MP/TCD instrument. Prior to analysis, the samples were outgassed at 100 °C for 3 h (residual pressure lower than 10^{-6} Torr). Apparent surface areas were determined by using Brunauer–Emmett–Teller equation (BET), in the relative pressure

Please cite this article in press as: C. Bisio, et al., Nanosized inorganic metal oxides as heterogeneous catalysts for the degradation of chemical warfare agents, Catal. Today (2016), http://dx.doi.org/10.1016/j.cattod.2015.12.023

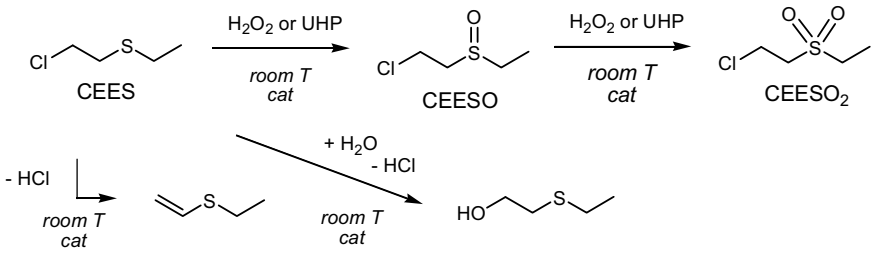

Scheme 1.

range from 0.01 to 0.1 P/P_0. Pore size distributions were obtained by applying the Non Local Density Functional Theory (NLDFT) method.

2.4. Catalytic tests

The first series of tests of catalytic oxidative abatement of the blistering agent simulant (2-chloroethyl) ethyl sulfide (CEES; Aldrich; 98%; Scheme 1) was performed as follows: a 14 mM solution of CEES in *n*-heptane (HPLC grade; Fluka) was reacted in a round-bottom glass batch reactor, at 298 K, in the presence of 30 wt% aqueous hydrogen peroxide (70 mM; Sigma–Aldrich) and 20 mg of solid catalyst. The total volume of the mixture was 20 mL. Samples of the reaction mixture were withdrawn at regular intervals (from 0 to 24 h). The CEES conversion was monitored by UV–Vis spectroscopy in transmission mode (1 mL quartz cuvette) on a PerkinElmer Lambda 900 spectrometer by monitoring the characteristic absorption maximum at 206 nm. The distribution of products and by-products was checked by GC–MS analysis on an Agilent 7890 Series gas-chromatograph equipped with MS detector (Supelco-5 ms column, 30 m × 0.25 mm; *n*-decane as internal standard). Blank tests were run in the absence of solid catalysts. Standard deviations of ±4%, ±5% were estimated, on average, for conversion and selectivity values, respectively. Product quantification and identification was also checked by ^{1}H NMR (300 MHz NMR Bruker Analytische Messtechnik GmbH), monitoring the peculiar signal of —CH_2—S of CEES, —CH_2—S=O of the sulfoxide (CEESO) and —CH_2—SO_2 of the sulfone ($CEESO_2$) in the range between 3.75 and 2.80 ppm [38].

The second series of tests for the catalytic oxidative decontamination of (2-chloroethyl) ethyl sulfide was performed as follows: a 100% cotton textile (9 cm^2; 200 mg ±10%) was impregnated with CEES (0.17 mmol) and immediately covered by the catalyst/UHP mixture (10 mg of solid mixture, containing 5 mg of catalyst and 5 mg of urea hydrogen peroxide solid, UHP, adduct (Fluka, 15–17% active oxygen basis)). After 5 minutes the cotton sheet was brushed and rinsed with 20 μL of deionized water. The decontamination efficiency was quantified in percentage by means of an on-field hazardous gas and chemical detector based on Open Loop Ion Mobility Spectrometry (CHEMPRO100*i*, Environics Oy). The off-vapours from the textile support were collected 2 cm above the contamination test area. The qualitative and quantitative analysis of the vapours has been performed according the CWA-High Sensitive (11.3.7), CWA-Sensitive (11.3.7) and First Responder (9.3.6) internal libraries, with respect to a non-treated control taken as 100% of the instrument output. Control tests were run in the absence of solid catalysts and/or in the absence of the chemical agent simulant.

2.5. Biological tests

The environmental biotoxicity of the catalysts was studied by bioluminescence inhibition tests, including determination of acute and chronic effects. Luminescent bacteria strain *P. leiognathi* Sh1, isolated from Azov Sea shrimp [39], was used as a biological target.

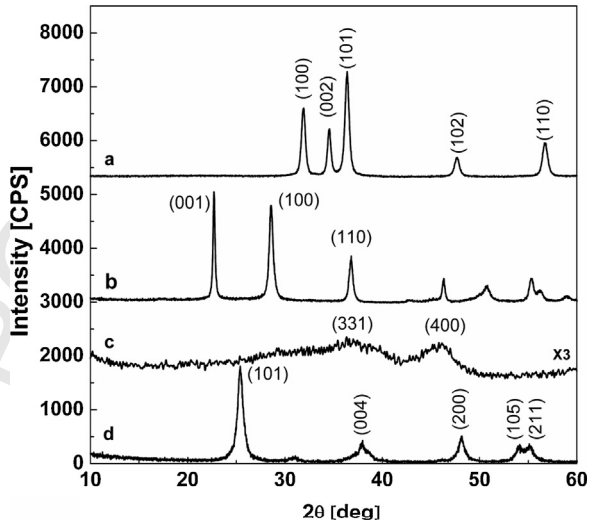

Fig. 1. XRD patterns of ZnO (a), Nb_2O_5 (b), γ-Al_2O_3 (c) and TiO_2 (d) samples. Q8

For the measurements, the overnight bacterial culture, grown in liquid nutrition medium (Nutrient Broth, Himedia, containing 3 wt% of NaCl), was diluted 100 times with aqueous 3 wt% sodium chloride solution. Reaction mixture for the determination of acute toxicity contained 850 μL of testing suspension in 3.0 wt% of sodium chloride solution mixed with 100 μL of 0.1 M phosphate buffer solution (pH 7.0) and 50 μL of diluted bacterial culture. The changes of bioluminescence were recorded within 10–30 min at 25 °C by using a bioluminometer BLM 8801 (Russia). In the case of chronic biotoxicity study, the reaction mixture, described above, additionally contained 50 μL of liquid nutrition medium and bioluminescence intensity was measured after 18 h of incubation at 25°C.

3. Results and discussion

3.1. Catalysts characterization

The structural properties of the catalysts were evaluated by powder X-ray diffraction (XRPD) technique. The XRPD profiles of the ZnO sample shows diffraction peaks at 31.8, 34.4, 36.6,47.6 and 56.7° 2θ, directly ascribed to the (1 0 0), (0 0 2), (1 0 1), (1 0 2) and (1 1 0) planes, typical of the wurtzite structure (Fig. 1a) [40].

The average particle diameter (L) of the ZnO sample was estimated by applying to the (1 1 0) peak the Debye–Scherrer equation (1), where B is the full width at half the maximum intensity (FWHM) of the (1 1 0) peak, λ is the X-ray wavelength, θ represents the diffraction angle and K is the Scherrer's constant (K = 0.89 for spherical particles).

$$B\left(2\theta\right) = \frac{K\lambda}{L\cos\theta} \quad (1)$$

The particle size of the ZnO sample was 13.8 nm.

The X-ray profile of Nb_2O_5 is composed of sharp peaks, indicative of a high crystallinity degree (Fig. 1b). The main reflections at 22.6, 28.5 and 36.9° 2θ, ascribed to the (0 0 1), (1 0 0) and (1 0 1) planes, respectively, are attributed to the hexagonal phase, according to the JCPDS Card no. 28–0317 [41]. The sample was composed of nanoparticles with size around 20 nm, as determined by the Debye–Scherrer equation applied to the (1 0 0) reflection.

The diffraction pattern of γ-Al_2O_3 shows a wide band centred at 38°2θ and two reflections at 46° and 66° 2θ, respectively due to (4 0 0) and(4 4 0) reflections of a γ-Al_2O_3 phase (Fig. 1c), thus suggesting that the heating treatment was effective to promote the phase transformation of boehmite into γ-alumina [42]. The reflections appear broad and poorly resolved and this is likely associated to the fact that the sample here prepared was composed by nanoparticles, below 10 nm, as estimated by TEM analysis (see below).

The XRPD profile of TiO_2 (Fig. 1d) is characterized by the peaks at 25.4, 37.8, 48.0, 54.1 and 55.1° 2θ, related respectively to the (1 0 1), (0 0 4), (2 0 0), (1 0 5) and (2 1 1) planes of the anatase phase (JCPDS 21–1272) [43]. The Debye–Scherrer equation applied to (1 0 1) plane allows estimating the particles size, which resulted to be 11.2 nm.

The morphology and particles shape of the catalysts were investigated by high-resolution transmission electron microscopy (HR-TEM). The ZnO sample is composed of crystals with layered morphology, well organized in a porous structure whose pore dimensions are dependent on the synthetic procedure (Fig. 2A). The layered morphology of the sample was also assessed by scanning electron microscopy images reported in a previous manuscript by some of us [40]. This porous structure results from the interconnection of ZnO grains and is typical of solids prepared at relatively low temperature (below 773 K) [36]. TEM analysis was also used to estimate the size and shape of the alumina nanoparticles (Fig. 2B). This analysis indicated that γ-Al_2O_3 sample is characterized by the presence of aggregates (flake-like) that are composed by small nanoparticles of ca. 5–10 nm with rod-like shape. Finally, TEM images of TiO_2 catalyst show aggregates composed by particles with not well defined shape and high crystallinity with size around 10–15 nm (Fig. 2C), in agreement with the XRPD results. Probably, the sonication process assisting the synthesis and the slow addition of water, aiming at promoting the hydrolysis and condensation of the titanium precursor, were responsible of the high crystallinity of the obtained TiO_2.

The textural features of all catalysts, in terms of specific surface area (SSA) and pore size distribution (PSD), were also investigated by N_2 physisorption experiments. ZnO shows an adsorption–desorption isotherm corresponding to the so-called "type III" in the Brunauer classification. A hysteresis loop "H3" is observed for the sample, associated to the presence of slit-shaped pores, relative to the formation of interspaces between the nanosheets, according to TEM analysis. The SSA, estimated by the BET equation, resulted to be 37 $m^2\ g^{-1}$, with a PSD centred at 5.0 nm (estimated by NLDFT method) and pores volume of 0.17 $cm^3\ g^{-1}$ (Table 1). γ-Al_2O_3 and TiO_2 nanoparticles showed similar adsorption isotherms of type "IV", with an hysteresis loop of "H3" type, typical of the presence of disordered pores whose shape is not well defined. This porosity is probably due to particle aggregation [44]. The γ-Al_2O_3 sample shows a SSA of 450 $m^2\ g^{-1}$ and large PSD centred at 5.4 nm, whereas the TiO_2 material was characterized by a SSA of 162 $m^2\ g^{-1}$ and PSD centred at 6.0 nm and pores volume of 0.30 $cm^3\ g^{-1}$ (Table 1).

Table 1
Textural features of the catalysts.

	Specific surface area (SSA) ($m^2\ g^{-1}$)	Pores size distribution (PSD) (nm)	Pores volume ($cm^3\ g^{-1}$)
ZnO	37	5.0	0.17
γ-Al_2O_3	450	5.4	0.50
TiO_2	162	6.0	0.30
Nb_2O_5	4.3	n.d.	n.d.

n.d.: not determined.

Nb_2O_5 is characterized by a type "II" isotherm without an appreciable hysteresis loop. The specific surface area was 4.3 $m^2\ g^{-1}$, a very low value if compared with previous samples (Table 1).

3.2. Catalytic tests

The catalytic properties of the samples were evaluated in the oxidative abatement of the blistering agent simulant (2-chloroethyl) ethylsulfide, CEES (Scheme 1), whose chemical reactivity is similar to sulfur mustard (blistering warfare agent, HD, according to the NATO code), but with a far reduced toxicity [45].

The first set of experiments was carried out in a batch reactor, under very mild conditions, at 298 K and at ambient pressure, in the presence of 30 wt% aqueous H_2O_2 (70 mM) in *n*-heptane and 20 mg of catalyst. The degradation reaction of CEES (14 mM) was followed by monitoring the main UV absorption of the substrate, at 206 nm. The test was also performed without catalyst and in the presence of H_2O_2 (blank test). In this case, CEES showed a negligible self-decomposition (a maximum of 4 mol% degradation after 24 h). When the catalysts were introduced, a marked CEES abatement was observed (Fig. 3). In particular, a progressive decrease of the CEES concentration was recorded in reasonable times, performing the reaction in the presence of γ-Al_2O_3, ZnO, TiO_2 and Nb_2O_5 materials. The degradation was remarkable during the first 2 h of reaction.

The TiO_2 catalyst was responsible for 44% of CEES abatement after 6 h and of 58% after 24 h. The moderately good performance

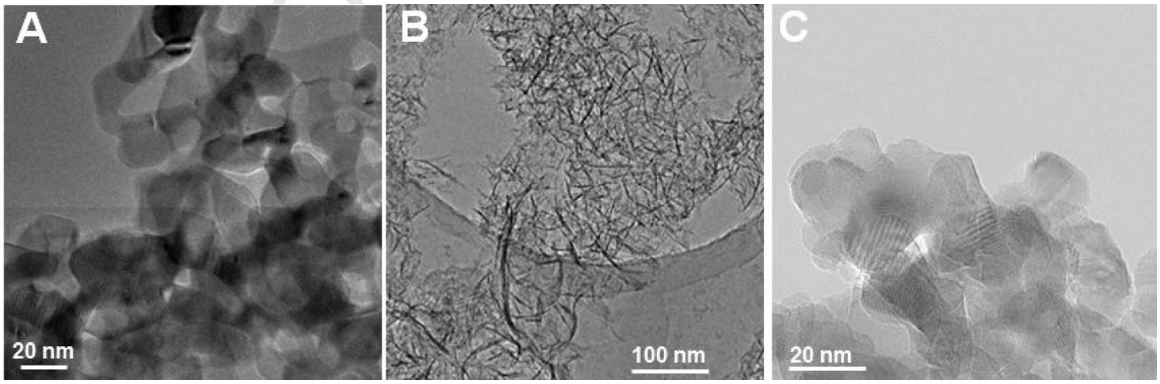

Fig. 2. HR-TEM micrographs of ZnO (A), γ-Al_2O_3 (B) and TiO_2 (C) samples.

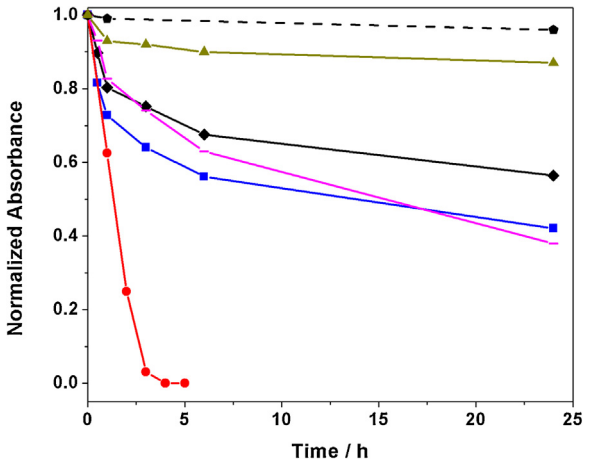

Fig. 3. Profiles of oxidative abatement of CEES with hydrogen peroxide over Nb_2O_5 (red), TiO_2 (blue), γ-Al_2O_3 (black), ZnO (purple), M75 decontamination powder (green, test without added H_2O_2) and without solid catalyst (dashed black). Reaction conditions: 14 mM CEES; 70 mM 30% aq. H_2O_2; *n*-heptane; 20 mg catalyst; 298 K. (For interpretation of the references to color in this figure legend, the reader is referred to the web version of this article.)

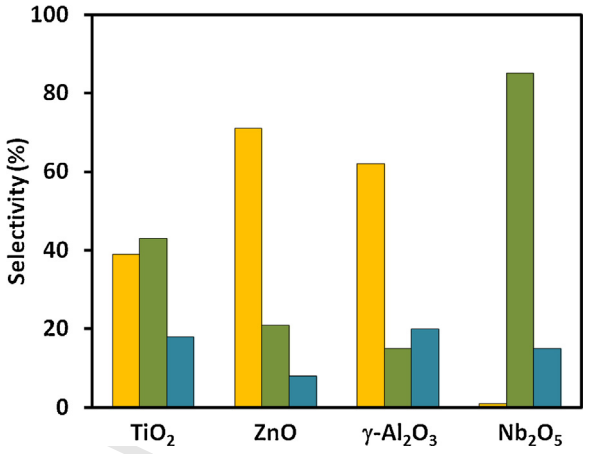

Fig. 4. Distribution of products in the oxidative abatement of CEES with hydrogen peroxide over Nb_2O_5, TiO_2, γ-Al_2O_3 and ZnO. Selectivity values to sulfoxide (CEESO; yellow), to sulfone ($CEESO_2$; green) and to other compounds (blue) were all taken at 35–40% conversion of CEES (at different reaction times). Reaction conditions: 14 mM CEES; 70 mM 30% aq. H_2O_2; *n*-heptane; 20 mg catalyst; 298 K. (For interpretation of the references to color in this figure legend, the reader is referred to the web version of this article.)

obtained in the presence of TiO_2 can be ascribed to the peculiar properties of this solid, that is capable to act via a hydrolytic pathway (with the elimination of HCl to provide (2-hydroxyethyl) ethylsulfide) as well as via an oxidative one (via the oxidation of the sulfide by hydrogen peroxide to sulfoxide and sulfone) [29,46,47]. It is worth underlining that the reaction took place over an anatase phase of TiO_2, which often leads to the unproductive disproportionation of H_2O_2 into oxygen and water [48]. However, thanks to the presence of an excess of oxidant (5:1 mol/mol ratio H_2O_2:CEES) in these tests, residual amounts of H_2O_2 have been always detected by iodometric tests, thus confirming that the oxidant was not the limiting agent in the reaction.

A similar behavior was observed for ZnO sample, though the degradation of CEES over this catalyst was a bit slower (37% of abatement after 6 h, Fig. 3). The capability of ZnO to degrade organic sulfide CWAs via non-photochemical pathways has already been described previously [49,50]. It was shown that the SSA of zinc oxide is an important factor to provide a good abatement rate. In addition, ZnO does not possess a proper oxidising ability, as it is the case for titanium dioxide samples. The low surface area and the negligible oxidising capacities of the present ZnO sample were thus likely the factors limiting the activity of this solid.

γ-Al_2O_3 shows an intermediate catalytic initial activity (within the first 2 h of reaction) with a conversion of 44% after 24 h, ascribable to the medium-strong Lewis acidity of the Al(δ^+) sites exposed on the surface (Fig. 3). In addition, in the present case, the small particles size and high specific surface area favoured a higher interaction between the catalyst and CEES substrate (see below). Similarly to ZnO, most of the catalytic activity of the aluminum oxide is to be related to its capability of promoting the chemical degradation via a hydrolysis pathway, which was also responsible of the degradation of sulfur mustard agent into thiodiglycol [51].

Interestingly, Nb_2O_5 showed the best catalytic performances in terms of conversion, leading to the complete abatement of CEES (>99%) within 5 h (Fig. 3). Over this solid, the remarkable acidic and oxidising properties of the oxide played a key role in determining such high activity. Indeed, Nb(V)-based solid oxides have shown a remarkable Lewis acidity together with an outstanding capability to trigger the oxidising action of aqueous hydrogen peroxide [52,53]. In the field of CWA degradation, only Nb(V)-polyoxoniobates have shown unique alkaline reactivity for nerve agent decontamination, but via a completely different reaction pathway [54]. However, no studies have taken into consideration niobia so far, as a potential catalyst for the oxidative degradation of CWA and the results are thus particularly promising.

Finally, the series of inorganic oxides has been compared with M75, a commercially available decontamination powder in use by the Italian armed forces and considered as a reference decontamination tool. Such powder is composed of a solid mixture of bentonite (a natural occurring solid containing montmorillonite clay as major component), alumina and calcium hypochlorite. Since the oxidant component was already present in the mixture, no added hydrogen peroxide was needed in the tests. In general, the performance of the M75 powder was the poorest within the tested catalyst set and the low conversion after 24 h (ca. 14%) is to be attributed mainly to the modest adsorption capacity of the bentonite clay.

In terms of selectivity, under the tested conditions, two main products were observed: (2-chloroethyl) ethylsulfoxide (CEESO) and (2-chloroethyl) ethylsulfone ($CEESO_2$), both derived from the oxidation of the pristine sulfide (Scheme 1). Other compounds obtained by acid/base-catalysed degradation of CEES, mainly vinylethylsulfide (via HCl elimination) and (2-hydroxyethyl) ethylsulfide, were summarised under the entry "others" in Fig. 4.

Taking into account that CEESO is the least hazardous oxidation product, ZnO was the most selective catalyst to the desired sulfoxide, in the aim of an effective and useful CWA degradation system. Then, γ-Al_2O_3 gave rise to the highest amount of non-oxidised products (ca. 20% at 40% conversion after 24 h), among which vinylethylsulfide was the major component. Interestingly, the most active catalyst, Nb_2O_5, was also very selective, although towards the undesired sulfone. In fact, the high oxidising ability of this solid resulted in a rapid oxidation of the sulfide into $CEESO_2$, which is a product to be considered as hazardous as the pristine sulfide, form the toxicological point of view [45].

A second set of experiments was performed mimicking a real contamination situation, on a cotton textile (9 cm^2; 200 mg), in the presence of CEES (0.17 mM), and using a solid mixture of catalyst with the UHP adduct. UHP was chosen as an oxidant in this case, because it is the best option to have a "solid equivalent" of hydrogen peroxide for decontamination powders. The contaminated textile support was treated with the decontamination powder mixture, brushed, after an action time of 5 min, in order to remove the solid and rinsed with water, thus simulating a conventional on-site

Please cite this article in press as: C. Bisio, et al., Nanosized inorganic metal oxides as heterogeneous catalysts for the degradation of chemical warfare agents, Catal. Today (2016), http://dx.doi.org/10.1016/j.cattod.2015.12.023

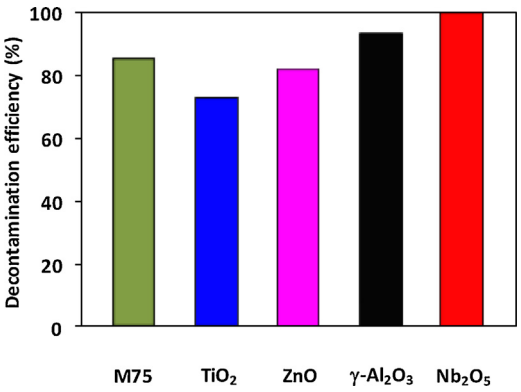

Fig. 5. Oxidative decontamination of CEES on textile with urea hydrogen peroxide. Decontamination efficiency with respect to a non-treated control (taken as 100%). Reaction conditions: 20 μL CEES; 10 mg catalyst/UHP mixture; 20 μL H_2O; brushing; 298 K.

immediate decontamination protocol. The effectiveness of CEES decontamination was monitored and quantified by means of an on-field CWA detector.

Remarkably, all tested catalyst led to an extensive decontamination from the sulfide in short time (Fig. 5). In terms of decontamination efficiency of the catalyst/oxidant mixtures, the following order was found: $Nb_2O_5 > \gamma\text{-}Al_2O_3 > ZnO > TiO_2$. The use of Nb_2O_5 and $\gamma\text{-}Al_2O_3$, in the presence of UHP, led to >98% and 92% CEES decontamination, respectively, after 5 min. These results are higher than the 85% conversion observed by using the reference M75 decontamination powder, currently in use. In particular, after treatment with the Nb_2O_5/UHP mixture, no residual contamination was detected by the on-field detector. ZnO and TiO_2, on the contrary, displayed a lower decontamination activity, but values as high as 82% and 73% were attained, respectively. In all cases, the oxidising capability of the powder is based on the use of a chlorine-free oxidant, UHP, instead of the environmentally unfriendly calcium hypochlorite. At the end of the decontamination tests, no hazardous levels of off-vapours were recorded on the textile support. That means that in none of the tests the degradation/decomposition by-products were revealed as toxic compounds above threatening levels by means of the on-field hazardous gas and chemical detector. Furthermore, this second series of results, collected on the cotton textile, showed that the abatement (oxidative degradation in a confined environment, under controlled conditions) and the decontamination properties (on-site degradation under total-loss conditions for the catalyst) of an oxidic material are not similar and cannot be considered fully comparable. In fact, the change in oxidant and reaction surroundings may exalt or diminish the decontamination efficiency of the nanostructured solids in the very short reaction times. For instance, the catalytic performances of $\gamma\text{-}Al_2O_3$ were particularly enhanced in the experiments on the textile, probably because of the cooperative positive effect of the high specific surface area, enabling a successful adsorption and physical removal of the contaminant, together with a good chemical degradation capability via in-situ hydrolysis, thanks to the acid character of its surface. Conversely, when a conventional Al_2O_3 solid, with micrometric particle size (Aldrich no. 19,997–4, Al_2O_3 activated, 155 $m^2\,g^{-1}$ specific surface area), was used under the same conditions, a remarkably lower decontamination capability was found: <10% vs. 92% of CEES decontamination efficiency, for the conventional Al_2O_3 and for the nanosized one, respectively. Various previous reports show indeed that inorganic oxides (Al_2O_3, MgO or hydrous zirconia) with a conventional non-nanostructured are scarcely active in adsorption plus degradation of organosulfur CWA analogues with respect to the nanosized oxide species [23,24,55]. On these systems, the contaminant is adsorbed, but the decontamination capability was ca. 20–25% only. Indeed, the nanometric size of the active inorganic oxide, that implies high surface area and a large number of catalytically active sites, is an important feature to have good properties of adsorption plus degradation [1,55].

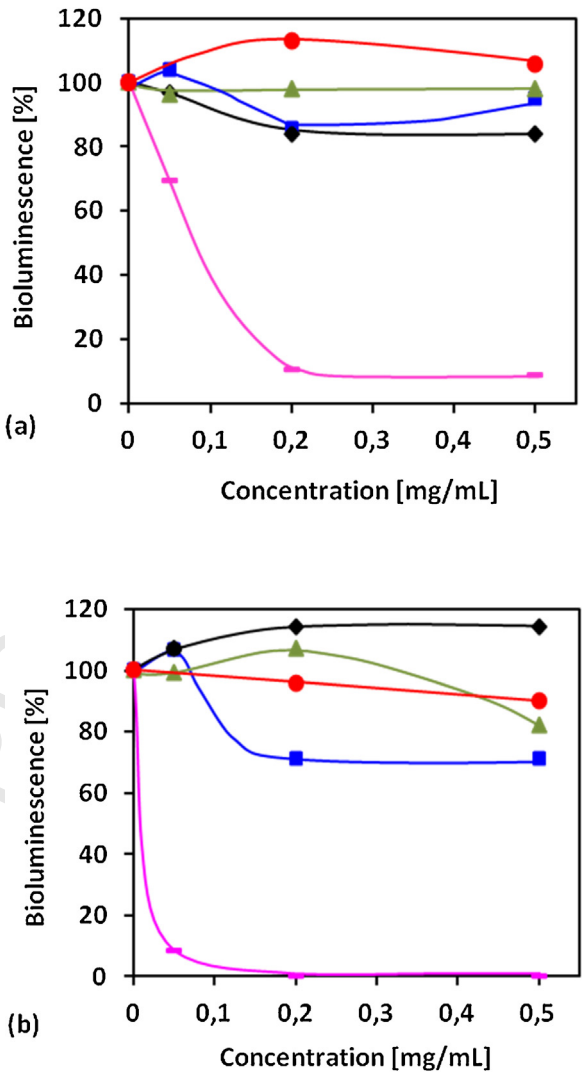

Fig. 6. Acute (a) and chronic (b) effects of decontaminating materials on *P. leiognathi* Sh1 bioluminescence. Nb_2O_5 (red), TiO_2 (blue), $\gamma\text{-}Al_2O_3$ (black), ZnO (purple), M75 decontamination powder (green). (For interpretation of the references to color in this figure legend, the reader is referred to the web version of this article.)

3.3. Environmental impact of the catalysts

The biological effects on the environment of the nanostructured oxidic catalysts have been estimated by means of bioluminescent bacteria biotests using a *P. leiognathi* Sh1 strain isolated from the Azov Sea [39]. Such methods are widely used to study the toxicity of chemicals, drugs and environmental objects, in general [56–58].

A direct comparison of the results of nanostructured oxides in the tests for acute and chronic toxicities did not reveal any significant difference. Indeed, strong acute and chronic inhibition effects on the glow of luminescent bacteria were revealed for the ZnO sample (Fig. 6a and b), which is widely known to possess marked antibacterial properties [59,60]. In particular, in the determination of the chronic toxicity, a complete suppression of the bacterial luminescence was revealed. Conversely, the rest of the solids as well as the reference conventional decontamination powder M75 did not show evident inhibition properties and did not have significant

detrimental effects on the bacterial luminescence. However, a weak inhibition activity of TiO_2 appeared and led to a 30% diminution of the luminescence. Analogously, the M75 powder presented a gradual chronic toxicity for concentrations higher than 0.2 mg mL^{-1}.

From these data, it is worth highlighting that Nb_2O_5, γ-Al_2O_3, M75 powder (notwithstanding the presence of hypochlorite salts in it) and, to a certain extent, TiO_2 did not show an evident environmental impact. ZnO, conversely, displayed a marked inhibition of the bacterial luminescence that is a clear evidence of its environmental negative impact.

4. Conclusions

A set of different tests, including the evaluation of abatement activity, decontamination capability and environmental impact, has been performed in order to have a comprehensive comparison of the performance for a series of nanosized inorganic metal oxides in the degradation of a simulant of blistering chemical warfare agent.

Niobium(V) oxide, Nb_2O_5, proved to be an extremely active, environmentally acceptable, although selective towards undesired by-products, catalyst in the degradation of CEES. Nevertheless, it gave excellent results in the on-site decontamination of CEES-contaminated cotton textile supports, showing that controlled abatements and on-site decontamination tests are not directly and readily comparable. ZnO, on the contrary, showed promising performances in terms of abatement activity and selectivity towards desired non-noxious products. However, it displayed a remarkable toxicity against environmental bacteria. Therefore, its use under total-loss conditions, as for decontamination purposes, is not advisable. TiO_2 showed an interesting activity under oxidative abatement conditions, even though its performance in on-site decontamination tests proved to be poorer than its conventional counterpart (commercial M75 powder). Finally, it is interesting to note that nanosized γ-Al_2O_3, prepared with a simple and fast preparation method, although is proved to be a moderate catalyst for the oxidative abatement of CEES, presented good selectivity to the non-noxious sulfoxide derivative and, in particular, with a remarkable decontamination capability thanks to its cooperative adsorption, oxidation and hydrolytic features.

All these considerations and the multidisciplinary merging of chemical, catalytic and biotesting evaluations can path the way towards the development of an environmentally-sustainable, active and selective inorganic nanostructured oxide solid catalyst for the safe degradation of highly hazardous chemical warfare agents.

Acknowledgements

Q6 The authors thank the NATO SPS Programme Multiyear Project "NanoContraChem" (no. 984481) for financial support. Technical support from Environics Oy, Finland, about the ChemPro100*i* detector is gratefully acknowledged. The authors are also grateful to Mr. Jacopo Sala and Ms. Laura Filippa for some experimental tests, and to Mr. Giorgio Cinquantini, from NBCsystem (Blera, Italy), for the fruitful technical discussion.

References

[1] K. Kim, O.G. Tsay, D.A. Atwood, D.G. Churchill, Chem. Rev. 111 (2011) 5345–5403.
[2] R.D. Albright, Cleanup of Chemical and Explosive Munitions, W. Andrew, Norwich, 2008.
[3] S. Popiel, Z. Witkiewicz, A. Szewczuk, J. Hazard. Mater. B 123 (2005) 94–111.
[4] G.W. Wagner, Ind. Eng. Chem. Res. 50 (2011) 12285–12287.
[5] R.D. Gall, C.L. Hill, J.E. Walker, J. Catal. 159 (1996) 473–478.
[6] N.M. Okun, T.M. Anderson, C.L. Hill, J. Mol. Catal. A: Chem. 197 (2003) 283–290.
[7] R. Raja, Top. Catal. 52 (2009) 322–332.
[8] J.M. Thomas, J.C. Hernandez, R. Raja, R.G. Bell, Phys. Chem. Chem. Phys. 11 (2009) 2799–2825.
[9] O.A. Kholdeeva, Catal. Sci. Technol. 4 (2014) 1869–1889.
[10] C.R. Ringenbach, S.R. Livingston, D. Kumar, C.C. Landry, Chem. Mater. 17 (2005) 5580–5586.
[11] S.R. Livingston, C.C. Landry, J. Am. Chem. Soc. 130 (2008) 13214–13215.
[12] D. Plachá, K. Rosenbergová, J. Slabotínský, K.M. Kutláková, S. Študentová, G.S. Martynková, J. Hazard. Mater. 271 (2014) 65–72.
[13] A. Michalkova, J. Martinez, L. Gorb, M. Ilchenko, O.A. Zhikol, O.V. Shishkin, J. Leszezynski, J. Phys. Chem. B 110 (2006) 21175–21183.
[14] F. Carniato, C. Bisio, R. Psaro, L. Marchese, M. Guidotti, Angew. Chem. Int. Ed. 53 (2014) 10095–10098.
[15] C. Tiozzo, C. Bisio, F. Carniato, A. Gallo, S.L. Scott, R. Psaro, M. Guidotti, Phys. Chem. Chem. Phys. 15 (2013) 13354–13362.
[16] M. Guidotti, R. Psaro, N. Ravasio, M. Sgobba, F. Carniato, C. Bisio, G. Gatti, L. Marchese, Green Chem. 11 (2009) 1173–1178.
[17] B. Singh, G.K. Prasad, K.S. Pandey, R.K. Danikhel, R. Vijayaraghavan, Def. Sci. J. 60 (4) (2010) 428–441.
[18] E. Lucas, S. Decker, A. Khaleel, A. Seitz, S. Fultz, A. Ponce, W. Li, C. Carnes, K.J. Klabunde, Chem. Eur. J. 7 (2001) 2505–2510.
[19] D.A. Panayotov, J.R. Morris, J. Phys. Chem. C 112 (2008) 7496–7502.
[20] S. Neatu, B. Cojocaru, V.I. Parvulescu, V. Somoghi, M. Alvaro, H. Garcia, J. Mater. Chem. 20 (2010) 4050–4054.
[21] Y. Zafrani, L. Yehezkel, M. Goldvaser, D. Marciano, D. Waysbort, E. Gershonov, I. Columbus, Org. Biomol. Chem. 9 (2011) 8445–8451.
[22] D.B. Mawhinney, J.A. Rossin, K. Gerhart, J.T. Yates, Langmuir 15 (1999) 4789–4795.
[23] R.S. Brown, J.A. Rossin, J.E. Kotary, G. Fitzgerald, K.G. Gerhart, H. Mearns, R.A. Newton, J.H. Keller, D.B. Mawhinney, J.T. Yates, US Patent no. 6, 852 (2005) 903.
[24] G.K. Prasad, P.V.R.K. Ramacharyulu, J.P. Kumar, K. Ganesan, B. Singh, J. Sci. Ind. Res. 71 (2012) 205–209.
[25] G.W. Peterson, J.A. Rossin, G.W. Wagner, US Patent no. 8, 530 (2013) 719.
[26] G.K. Prasad, P.V.R.K. Ramacharyulu, B. Singh, K. Batra, A.R. Srivastava, K. Ganesan, R. Vijayaraghavan, J. Mol. Catal. A: Chem. 349 (2011) 55–62.
[27] E. Lucas, S. Decker, A. Khaleel, A. Seitz, S. Fultz, A. Ponce, W. Li, C. Carnes, K.J. Klabunde, Chem. Eur. J. 7 (2001) 2505–2510.
[28] D.A. Trubitsyn, A.V. Vorontsov, J. Phys. Chem. B 109 (2005) 21884–21892.
[29] M.B. Mitchell, V.N. Sheinker, E.A. Mintz, J. Phys. Chem. B 101 (1997) 11192–11203.
[30] A. Kleinhammes, G.W. Wagner, H. Kulkarni, Y. Jia, Q. Zhang, L.C. Qin, Y. Wu, Chem. Phys. Lett. 411 (2005) 81–85.
[31] P.R. Gil, G. Oberdoester, A. Elder, V. Puntes, W.J. Parak, ACS Nano 4 (2010) 5527.
[32] T. Xia, M. Kovochich, M. Liong, L. Madler, B. Gilbert, H. Shi, J.I. Yeh, J.I. Zink, A.E. Nel, ACS Nano 2 (2008) 2121–2134.
[33] J.G. Reynolds, B. Hart, J. Mater. (2004) 36.
[34] M. Heinlaan, A. Ivask, I. Blinova, H.C. Dubourguier, A. Kahru, Chemosphere 71 (2008) 1308–1316.
[35] N.F. Starodub, K.E. Shavanova, M.V. Taran, A.M. Katsev, R.V. Son'ko, C. Bisio, M. Guidotti, Proc. SPIE 9421 (2014) 942106.
[36] K. Kakiuchi, E. Hosono, T. Kimura, H. Imai, S. Fujihara, J. Sol–Gel Sci. Technol. 39 (2006) 63–72.
[37] X. Bokhimi, J. Sánchez-Valente, F. Pedraza, J. Solid State Chem. 166 (2002) 182–190.
[38] X. Shi, W. Ma, H. Ou, X. Han, C. Lu, Y. Chen, J. Wei, J. Braz. Chem. Soc. 23 (8) (2012) 1536–1542.
[39] A.M. Katsev, Tavricheskiy Mediko-Biologicheskiy Vestnik 17 (2014) 59–64.
[40] D. Costenaro, F. Carniato, G. Gatti, C. Bisio, L. Marchese, J. Phys. Chem. C 115 (2011) 25257–25265.
[41] J. He, Y. Hu, Z. Wang, W. Lu, S. Yang, G. Wu, Y. Wang, S. Wang, H. Gu, J. Wang, J. Mater. Chem. C 2 (2014) 8185–8190.
[42] A. Sacco, A. Lamberti, M. Gerosa, C. Bisio, G. Gatti, F. Carniato, N. Shahzad, A. Chiodoni, E. Tresso, L. Marchese, Solar Energy 111 (2015) 125–134.
[43] J. Lu, L.P. Bauermann, P. Gerstel, U. Heinrichs, P. Kopold, J. Bill, F. Aldinger, Mater. Chem. Phys. 115 (2009) 142–146.
[44] S. Lowell, J.E. Shields, M.A. Thomas, M. Thommes, Characterization of Porous Solids and Powders: Surface Area Pore Size and Density, Springer, Dordrecht, 2004.
[45] J. Hirade, A. Ninomiya, J. Biochem. 37 (1950) 19–26.
[46] Y.C. Yang, L.L. Szafraniec, W.T. Beaudry, J.R. Wagner, J. Org. Chem. 53 (1988) 3293.
[47] G.W. Wagner, L.R. Procell, Y.C. Yang, C.A. Bunton, Langmuir 17 (2001) 4809–4811.
[48] U. Romano, M. Ricci, in: M.G. Clerici, O.A. Kholdeeva (Eds.), Liquid Phase Oxidation via Heterogeneous Catalysis: Organic Synthesis and Industrial Applications, John Wiley & Sons, 2013, pp. 453–454.
[49] V. Houskova, V. Stengl, S. Bakardjieva, N. Murafa, A. Kalendova, F. Oplustil, J. Phys. Chem. A 111 (2007) 4215–4221.
[50] G.W. Wagner, P.W. Bartram, O. Koper, K.J. Klabunde, J. Phys Chem. B 103 (1999) 3225–3228.
[51] G.W. Wagner, L.R. Procell, R.J. O'Connor, S. Munavalli, C.L. Carnes, P.N. Kapoor, K.J. Klabunde, J. Am. Chem. Soc. 123 (2001) 1636–1644.
[52] V. Lacerda, D. Araujo dos Santos, L. Carlos da Silva-Filho, S.J. Greco, R. Bezerra dos Santos, Aldrichim. Acta 45 (2012) 19–27.

Please cite this article in press as: C. Bisio, et al., Nanosized inorganic metal oxides as heterogeneous catalysts for the degradation of chemical warfare agents, Catal. Today (2016), http://dx.doi.org/10.1016/j.cattod.2015.12.023

[53] M. Ziolek, Catal. Today 78 (2003) 47–64.
[54] M.K. Kinnan, W.R. Creasy, L.B. Fullmer, H.L. Schreuder-Gibson, M. Nyman, Eur. J. Inorg. Chem. 14 (2014) 2318–2321.
[55] B.E. Lanz, M.W. Sigel, D.A. Jones, J.T. Rhule, R.S. Mulukutla, US Patent no. 2003/0215355 (2003).
[56] G.G. Berest, O.Y. Voskoboynik, S.I. Kovalenko, I.S. Nosulenko, L.M. Antypenko, O.M. Antypenko, V.M. Shvets, A.M. Katsev, Sci. Pharm. 80 (2012) 37–65.
[57] L.N. Antipenko, A.V. Karpenko, S.I. Kovalenko, A.M. Katsev, E.Z. Komarovska-Porokhnyavets, V.P. Novikov, Arch. Pharm. 342 (2009) 620–651. Q7
[58] F. Fernández-Piñas, I. Rodea-Palomares, F. Leganés, M. González-Pleiter, M. Angeles Muñoz-Martín, Adv. Biochem. Eng. Biotechnol. 145 (2014) 65–135.
[59] Y. Liu, L. He, A. Mustapha, H. Li, Z.Q. Hu, M. Lin, J. Appl. Microbiol. 107 (2009) 1193–1201.
[60] K.H. Tam, A.B. Djurišić, C.M.N. Chan, Y.Y. Xi, C.W. Tse, Y.H. Leung, W.K. Chan, F.C.C. Leung, D.W.T. Au, Thin Solid Films 516 (2008) 6167–6174.

Please cite this article in press as: C. Bisio, et al., Nanosized inorganic metal oxides as heterogeneous catalysts for the degradation of chemical warfare agents, Catal. Today (2016), http://dx.doi.org/10.1016/j.cattod.2015.12.023